Science in China Series D: Earth Sciences

www.scichina.com
earth.scichina.com
www.springerlink.com

The 20—30-day oscillation of the global circulation and heavy precipitation over the lower reaches of the Yangtze River valley

YANG QiuMing†

Jiangsu Meteorological Institute, Nanjing 210008, China

Based on the observational data in summer, the variations of intraseasonal oscillation (ISO) of the daily rainfall over the lower reaches of the Yangtze River valley (LYRV) were studied by using the non-integer spectrum analysis. The NCEP/NCAR reanalysis data for the period of 1979—2005 were analyzed by principal oscillation pattern analysis (POP) to investigate the spatial and temporal characteristics of principal ISO patterns of the global circulation. The relationships of these ISO patterns to the rainfall ISO and the heavy precipitation process over LYRV were also discussed. It is found that the rainfall over LYRV in May—August is mainly of periodic oscillations of 10—20, 20—30 and 60—70 days, and the interannual variation of the intensity of its 20—30-day oscillation has a strongly positive correlation with the number of the heavy precipitation process. Two modes (POP1, POP2) are revealed by POP for the 20—30-day oscillation of the global 850 hPa geopotential height. One is a circumglobal teleconnection wave train in the middle latitude of the Southern Hemisphere (SCGT) with an eastward propagation, and the other is the southward propagation pattern in the tropical western Pacific (TWP). The POP modes explain 7.72% and 7.66% of the variance, respectively. These two principal ISO patterns are closely linked to the low frequency rainfall and heavy precipitation process over LYRV, in which the probability for the heavy precipitation process over LYRV is 54.9% and 60.4% for the positive phase of the imaginary part of POP1 and real part of POP2, respectively. Furthermore, the models of the global atmospheric circulation for the 20—30-day oscillation in association with or without the heavy precipitation process over LYRV during the Northern Hemisphere summer are set up by means of the composite analysis method. Most of the heavy precipitation processes over LYRV appear in Phase 4 of SCGT or Phase 6 of TWP. When the positive phases of 20—30-day oscillations for the rainfall over LYRV are associated with (without) the heavy precipitation process, a strong westerly stream appears (disappears) from the Arabian Sea via India and Bay of Bengal (BOB) to southern China and LYRV for the global 850 hPa filtered wind field during Phase 4 of SCGT. This situation is favorable (unfavorable) for the forming of the heavy precipitation process over LYRV. Similarly, a strong (weak) western wind belt forms from India through BOB to southern China and LYRV and the subtropical northwestern Pacific and central and eastern equatorial Pacific during Phase 6 of TWP for the cases with (without) the heavy precipitation process. The evolutions of these ISO patterns related to the 20—30-day oscillation are excited by either the interaction of extratropical circulation in both hemispheres or the heat source forcing in Asia monsoon domain and internal interaction of circulation in East Asia. These two

Received January 15, 2009; accepted May 10, 2009
doi: 10.1007/s11430-009-0156-2
†Corresponding author (email: yqm0305@263.net)
Supported by the Program for the Fundamental Research of China Meteorological Administration (Grant No. 200726)

Citation: Yang Q M. The 20—30-day oscillation of the global circulation and heavy precipitation over the lower reaches of the Yangtze River valley. Sci China Ser D-Earth Sci, 2009, 52(10): 1485-1501, doi: 10.1007/s11430-009-0156-2

global circulation models might therefore provide valuable information for the extended-range forecast of the heavy precipitation process over LYRV during the 10—30 days.

20—30-day oscillation, heavy precipitation process over reaches of Yangtze River valley, principal oscillation pattern, global atmospheric circulation models, summer

Intraseasonal oscillation (ISO) is one of the most pronounced large-scale climate signals in the global atmospheric. In early 1970s, Madden and Julian[1,2] indicated the existence of tropical atmospheric ISO, i.e., MJO. Afterwards, the study on the tropical ISO has been unfolded vigorously since the 1980s, and the structural feature and basic active rule of the tropical ISO were well understood. On the other hand, the spatial and temporal variations of the mid-high latitudes ISO and its relationships to the tropical ISO have been widely investigated. The action and anomaly of these ISO patterns have great influences on the weather/climate variations in many parts of the world[3—16]. Recent studies show that the tropical ISO has an important impact on the tropical climate system, and its action and anomaly affect not only the onset and activity of Asian summer monsoon but also the occurrence of ENSO[17]. Moreover, the interaction between the tropical ISO and Antarctic Oscillation (AAO)[12] is significant. In addition, Mao et al.[18] used the data in the 1991 Meiyu period to study the effect of the 15—35-day oscillation of the subtropical high on the Yangtze-Huaihe River rainfall. He et al.[19] noted the influence of Australian cold air activity for the quasi-40 day oscillation on the rainfall over the low and middle reaches of the Yangtze River valley (LMYRV). These studies provided some important information for the medium-range forecast of the rainfall over LMYRV in summer. At present, the dynamical or statistical models are being used in real-time weather climate discussions and experimental week 2—4 predictions of the ISO and high-impact weather events (persistent heavy rainfall, high or low temperature, etc.)[20—28]. However, there are many questions on activity and influence of the ISO, such as the ISO associated with high-impact weather events, potential predictability of ISO, and we should further study them, particularly the effect of 20—30-day oscillations on the persistent heavy rainfall over the Yangtze River valley (YRV)[29,30].

The persistent heavy rainfall over YRV occurs against the background of weak summer East Asia monsoon, which is associated with the strong 20—30-day oscillation and is important for the maintenance of this heavy rainfall. The 20—30-day oscillation is favorable not only for the cold air currents at high latitudes in East Asia and tropical monsoon surge meeting and maintaining over YRV but also for the stronger activity of Rossby waves in the upper westerly jet stream in Asia, leading to the stronger Meiyu front and ascending motion. At the same time, a low frequency oscillation of the western Pacific subtropical high is favorable for the reproducing and maintaining of low pressure systems in YRV (115°—125°E)[29]. Many of the previous studies have mainly focused on the impacts of the 20—30-day oscillation in East Asia on the persistent heavy rainfall over YRV and the latitude-time Hovmoller plots to describe the origin and propagation features of these ISO patterns. But, there are few studies on the connections between the persistent heavy rainfall over YRV and the circulation anomalies in mid-high latitudes of the Southern Hemisphere on the time scale of 20—30 days. The circulations in extratropics in both hemispheres and the tropical convection influence the forming of the heavy precipitation process over YRV, and have an important interaction on the subseasonal time scales[31]. To understand the possible mechanisms for the summer heavy precipitation process and improve the prediction for the extended-range forecasting during the 10—30 days, it is important to realize and interpret the connections between the 20—30-day oscillation of the global circulations and heavy precipitation process in YRV.

The current work, with the daily NCEP/NCAR reanalysis data[32] and the summertime rainfall over the lower reaches of Yangtze River valley (LYRV), studies the variation of the low-frequency oscillation of daily rainfall over LYRV and the connections between the heavy precipitation process and the ISO patterns of the global circulation from May to August in the recent 27 years. And the methods of the non-integer spectrum analysis[33], correlation analysis, and POP analysis[34,35] are applied to study the temporal and spatial characteris-

tics of the ISO patterns and their relationships. Furthermore, the models of the global atmospheric circulation for 20—30- day oscillations in association with or without the heavy precipitation process over LYRV in May—August are set up by means of the composite analysis method, and the difference of the global atmospheric circulation associated with the different ISO patterns is also discussed.

1 Data and methods

The global sea level pressure, geopotential height, wind field and outgoing longwave radiation (OLR) for the years 1979—2005 were used from the National Centers for Environmental Prediction/National Center for Atmospheric Research (NCEP/NCAR) for the grid daily reanalysis data (2.5°×2.5°). The summertime year (May 1 through August 31) is selected for the 27 years from 1979 to 2005, and the length of the annual series is 123 days, which was availability of better and more reliable data quality for the post-1978 data, particularly the global reanalysis data of NCEP/NCAR over the Southern Hemisphere. The daily precipitation data in LYRV (average of the 25 stations for the region (118.0°—122.5°E, 30.5°—32.0°N)) were also selected for the period of 1961—2005. And the daily anomalous series were obtained for all data.

A non-integer spectrum analysis power spectral analysis[33] was performed on a yearly basis to study the variation of the low frequency oscillation of daily precipitation over LYRV in May—August. Then, the teleconnections between the low frequency rainfall over LYRV and the global circulations were analyzed, and the global principal ISO patterns were revealed by POP[34—36] for the global 850 hPa geopotential height anomalies on the time scale of 20—30 days. We studied the correlations between its time coefficients and low frequency rain over LYRV and performed statistical analysis of the probability of the heavy precipitation process over LYRV for the positive or negative phases of principal intraseasonal oscillation patterns in the recent 27 years. Moreover, the models of the global atmospheric circulation for the 20—30-day oscillation in association with or without the heavy precipitation process over LYRV in May—August were also set up by means of the composite analysis method. Meanwhile, the evolutions of the 20—30-day oscillation for the OLR associated with the principal ISO patterns were analyzed. Additionally, the test of significance for the correlation considered the inherent persistence in filtered series, in which the effective numbers of independent samples were estimated[37].

POP analysis is a diagnostic tool employed to infer the space-time characteristics of a complex, dynamical system[34,35]. To understand the origin and propagative features of the intraseasonal modes, POP analysis was applied. POP analysis has been successfully used to understand the propagative features of the MJO and ENSO[35]. In the present study, we follow a similar procedure as described in Hasselmann[34] and von Storch et al.[35] in constructing the POP cycle for the global 850 hPa geopotential height. A brief description is provided here and the details are in the review article of von Storch et al.[35]. The procedure involves three parts. First, a set of the principal component analysis (PCA) is constructed from the state space (filtered data) that retains more than 60% of the variance. Secondly, a linear model (Markov model), similar to a single step autoregressive model, is computed using this reduced state space. Finally, POPs, which are independent modes of this Markov model, are calculated. The real and imaginary time coefficients associated with the POP patterns are used to produce the POP cycle, which provide insight into the origin and propagating features of the global principal ISO patterns.

2 Relationship between the low-frequency oscillation of rainfall and the heavy precipitation process over LYRV

2.1 Variation of the low-frequency oscillation of rainfall over LYRV during the period of 1961—2005

To better understand the low-frequency oscillatory variation of rainfall over LYRV, a non-integer spectral analysis[33] of the daily rainfall for May 1—August 31 in 1961—2005 is performed. Figure 1 gives a 95% significance level test of two-dimensional non-integer power spectra (statistical parameter F>3.50) for the regression equation corresponding to the non-integer period, with the individual periods (non-integer) as the abscissa and the time (year) as the ordinate. It is seen that the primary periods that have statistical significance at a 95% confidence level are of 10—20 days, 20—30 days, and 60—70 days. The 20—30-day oscillations are less significant in the mid-1960s and 1990s than in other time. The periodic oscillations of 10—20 days are mainly in the early

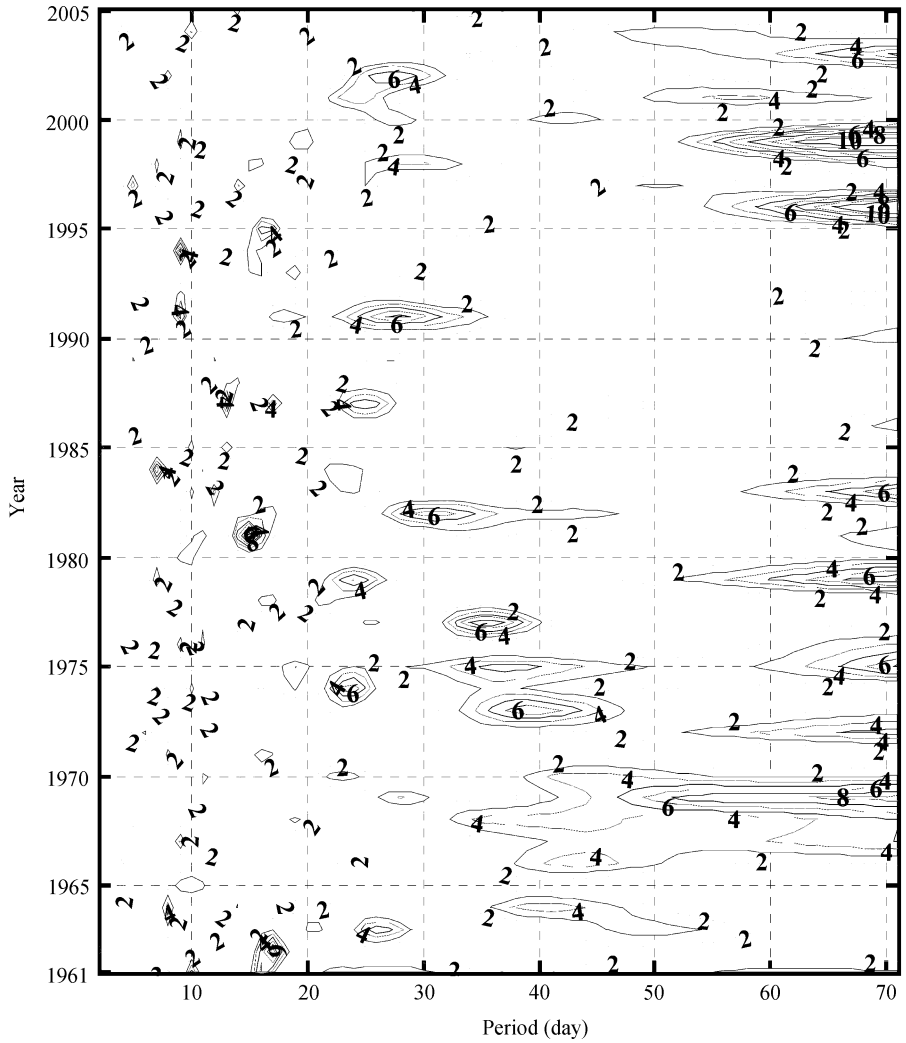

Figure 1 Interannual variations of the periods for the daily rainfall over the lower reaches of Yangtze River valley (LYRV) in May—August during the period of 1961—2005. Shaded values are significant at 95% confidence level.

1960s and the time from the 1980s to the end of 1990s. The periodic oscillations of 60—70 days are statistically significant at a 95% confidence level from the late 1960s to 1984 and the late 1990s to the present, but are not significant from the mid-1980s to 1990s. Besides, there is a significant periodic oscillation of 30—50 days from the 1960s to the early 1980s. Therefore, it can be now concluded that the summertime rainfall over LYRV is mainly displayed as the periodic oscillations of 10—20 days, 20—30 days, and 60—70 days.

2.2 Relationship between the interannual intensity variation of low-frequency oscillation of rainfall and the number of the heavy precipitation process over LYRV

The variation of the low frequency oscillation of the rainfall has an important influence on the heavy precipitation process. Figure 2(a) shows the interannual variations of the number of the heavy precipitation process over LYRV (average of daily precipitation in this region is greater than or equal to 25 mm) in May—August from 1961 to 2005. Similarly, the non-integer spectral analysis is also conducted for this time series. It is found that the variation of the number of the heavy precipitation process over LYRV is mainly of oscillations of 2.0 and 11.2 years, but the long-range trend is less significant.

To study the relationships between the interannual intensity variation of the low-frequency oscillation of rainfall over the different ranges of frequency and the number of the heavy precipitation process over LYRV, the correlation coefficients are computed between the statistical parameter F series (Figure 1) corresponding to

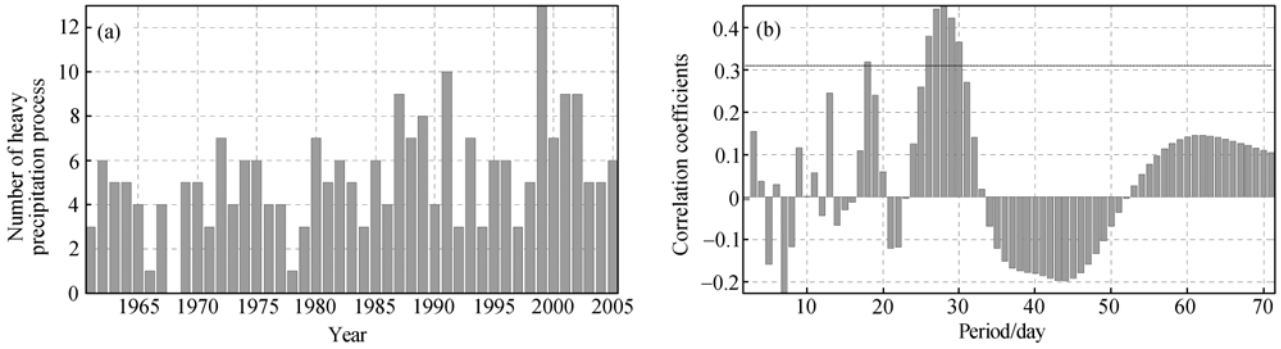

Figure 2 (a) Time series of the number of the heavy precipitation process over LYRV in May—August from 1961 to 2005. (b) Correlations between the number of the heavy precipitation process and the intensity of the periods on the time scale of 10—70 days, in which the significant level of 95% is represented by horizontal dashed line.

the individual periods (non-integer) and the number of the heavy precipitation process over LYRV in May—August. It is used here to analyze the time series from 1961 through 2005. Figure 2(b) displays the correlations between the number of the heavy precipitation process and intensity of the periods on the time scale of 10—70 days. It follows that the number of heavy precipitation process over LYRV has a strongly positive correlation with the intensity of its 28-day oscillation (with the correlation coefficient of 0.452 and statistically significant at a 99% confidence level). And it has a significantly positive correlation with that of the 18-day oscillation (with the correlation coefficient of 0.319 and statistically significant at a 95% confidence level), but has an insignificant relationship with that of the 30—70-day oscillation. It is then concluded that the variations of the intensity of the 20—30-day and 10—20-day oscillations have a significantly positive correlations with the heavy precipitation process over LYRV. The strong and weak years of these two oscillations are associated with normal to anomalously more and normal to anomalously less number of the heavy precipitation process over LYRV. These relationships are of indicative guidance for the climatic prediction of the heavy precipitation process over LYRV. Therefore, it is realistically important to work hard on improving the study on the 20—30-day and 10—20-day oscillations of rainfall over LYRV and their connections to the principal circulation patterns on the subseasonal time scales.

Since the relationship between the intensity of the 20—30-day oscillation of daily rainfall and the number of heavy precipitation process over LYRV is the most significant, the evolution of the 20—30-day oscillation would provide a better indicative significance for the extended-range forecasting during the 10—30 days. In this study, we focus mainly on the possible links between the rainfall and circulation oscillations on the time scale of 20—30 days.

3 Global atmospheric circulation models with and without the heavy precipitation process over LYRV for the global principal intraseansonal oscillation patterns on the time scale of 20—30 days

3.1 Teleconnection between the 20—30-day oscillation of the rainfall over LYRV and the global atmospheric circulation

To isolate the variations related to the 20—30-day modes, we chose the time series of the global sea level pressure, 850 hPa, 700 hPa, 500 hPa, 300 hPa, 200 hPa, and 100 hPa geopotential height anomalies from May to August during the period of 1979—2005, 123 days each year, i.e., 3321 days. These time series were dealt with the 20—30-day band pass filtering (Butterworth filtering[38]) and standardized. Then we applied separately PCA to study spatial and temporal distributions of ISO patterns. From correlations between the low frequency rainfall of LYRV on the time scale of 20—30 days and these principal components, we found that the connection to the 850 hPa geopotential height is the most significant. The correlations between the low frequency rainfall over LYRV and the first five principal components for 850 hPa geopotential height are 0.117, –0.224, 0.079, 0.023, and 0.037, respectively. The correlation of that to the second principal component is –0.224, which

is statistically significant at a 95% confidence level from a 2-tailed Student's *t*-test (the effective number of independent samples is 130 days). Therefore, we mainly study the effect of the global ISO patterns for the 850 hPa geopotential height on the rainfall ISO and the heavy precipitation process over LYRV on the time scale of 20—30 days.

Figure 3(a) shows the spatial distribution of ratio of the standard deviation for the 20—30-day signal to the total variability for the 850 hPa geopotential height in May—August. It follows that the areas of the larger variance contribution of ISO are distributed over the mid-high latitudes in Eurasia continent and North America continent and the Southern Hemisphere, tropical western Pacific, central Pacific, northern Indian Ocean and subtropical northern Atlantic. And the maximum centers are over the middle latitude of southern Pacific, northern part of northeastern Asia, and northern Canada, where the values in these centers exceed 30%. This indicates the existence of a pronounced

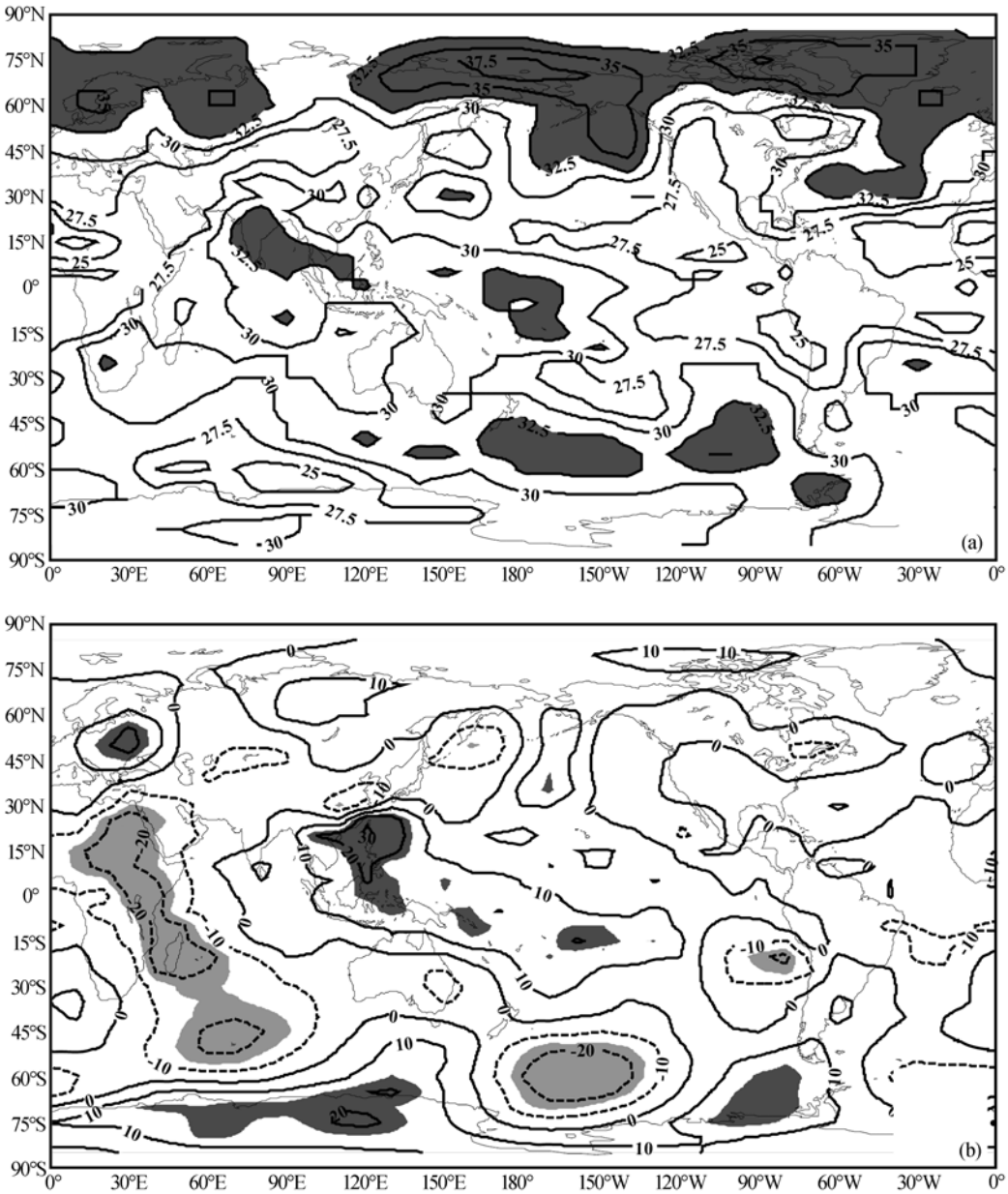

Figure 3 (a) Spatial distribution of ratio of the standard deviation for the 20—30-day signal to the total variability, whose values (unit: %) are multiplied by 100 and the contours greater than or equal to 32.5 are shaded; (b) teleconnections between the 20—30-day low-frequency rainfall over LYRV and global 850 hPa low frequency height anomalies. Values are multiplied by 100. Above 95% confidence level is shaded.

20—30-day oscillation for the atmospheric circulation in May—August, which is global in nature. Furthermore, Figure 3(b) gives the teleconnections between the 20—30-day low frequency rainfall over LYRV and the global 850 hPa low frequency height anomalies. In calculation, the effective number of independent samples is found to be approximately 133 days, averaged for all the grid points. The correlations of 0.171 and 0.223 indicate significance levels of 95% and 99%, respectively. Figure 3(b) clearly shows that the highly positive correlation regions concentrate on the southeastern China, tropical western Pacific, and central Europe, in which the most significant is over the tropical western Pacific with the 99% significance level. And the significantly negative correlations are also seen over at the mid-high latitudes in the southern Pacific and the region from northern Africa through eastern Africa to the middle latitude of the southern Indian Ocean, respectively. These regions are statistically significant at a 95% confidence level. Above the negative region over from East Africa to the southern Indian Ocean is located near the region for the Somali jet associated with South Asia summer monsoon, which reflects the connection between the cross- equatorial flow in this region and rainfall over LYRV on the time scale of 20—30 days. Thus, a correlation between the low frequency rainfall over LYRV and circulations of the tropical western Pacific is significant. And a teleconnection of that to the circulations of the mid-high latitudes in the Southern Hemisphere also tends to be strong. This teleconnection is likely related to the interaction in both hemispheres on the time scale of 20—30 days.

In what follows, we endeavor to find the temporal and spatial variations of the principal ISO patterns of the global 850 hPa geopotential height and the evolutions of the global circulation models related to the rainfall ISO and the heavy precipitation process over LYRV in May—August.

3.2 Global principal intraseansonal oscillation patterns and their relationships to the heavy precipitation process over LYRV on the time scale of 20—30 days

The POP analysis is applied to the filtered global 850 hPa daily geopotential height anomalies with a 20—30-day for May—August of each year. The spatial patterns of the real (p_r) and imaginary (p_i) parts of the dominant POP1 (Figure 4(a) and (b)), POP2 (Figure 5(a) and (b)) mode, and the two POP coefficient time series $z_r(t)$ and $z_i(t)$ (not shown) corresponding to these spatial patterns are identified. These two POP modes explain 7.72%, 7.66% of the variance and have a rotation period of about 25.9, 29.7 days and a decay/damping time of about 217.4, 96.0 days, respectively. Correspondingly, the POP cycle consists of: $\cdots \rightarrow p_i \rightarrow p_r \rightarrow -p_i \rightarrow -p_r \rightarrow p_i \rightarrow \cdots$.

The real part of POP1 mode shows a pronounced circumglobal wave train with signs changing alternatively over the mid-high latitudes of the Southern Hemisphere in Figure 4(a); while the imaginary part, which occurs a quarter of the rotation period before the real part (i.e., in about 7 days), also appears a similar wavetrain (Figure 4(b)). It is evident from the POP cycle that there is a remarkable wavetrain associated with an eastward propagating ISO along the westerly jet stream over the middle latitude of the Southern Hemisphere. This mode is defined as the southern circumglobal teleconnection wave train (SCGT), similar to the results of refs. [39, 40]. It is closely linked to the internal nonlinear interactions of the extratropical atmospheric circulation in the Southern Hemisphere. For this mode, the significant regions of the explained variance concentrate on the extratropics in the Southern Hemisphere (Figure 4(c)) and maximum center, up to 15%, is to the southeastern Pacific Ocean coast of South America. Another interesting feature is that there is a prominent negative value belt from southern Europe via Center East to northwestern China in the real part (Figure 4(a)). This spatial pattern represents the peak phase of the developing stage of the geopotential height disturbance in the middle latitude in Eurasia in the POP cycle, with the explained variance greater than 5% (Figure 4(c)). The existence of the active region above suggests the relationship of the disturbed westerly jet stream in the middle latitude of the Southern Hemisphere to the circulation in the southern part of Eurasia continent. This connection may be responsible for the interaction in both hemispheres. It indicates that the 20—30-day oscillation of SCGT has an indirectly remarkable impact on the East Asia summer monsoon and climate in LYRV. However, this possible mechanism needs to be further studied.

For the POP2 mode, the spatial patterns of the real and imaginary parts are shown in Figure 5(a) and (b), respectively. Clearly, the spatial distribution is characterized by a wave train structure with signs changing

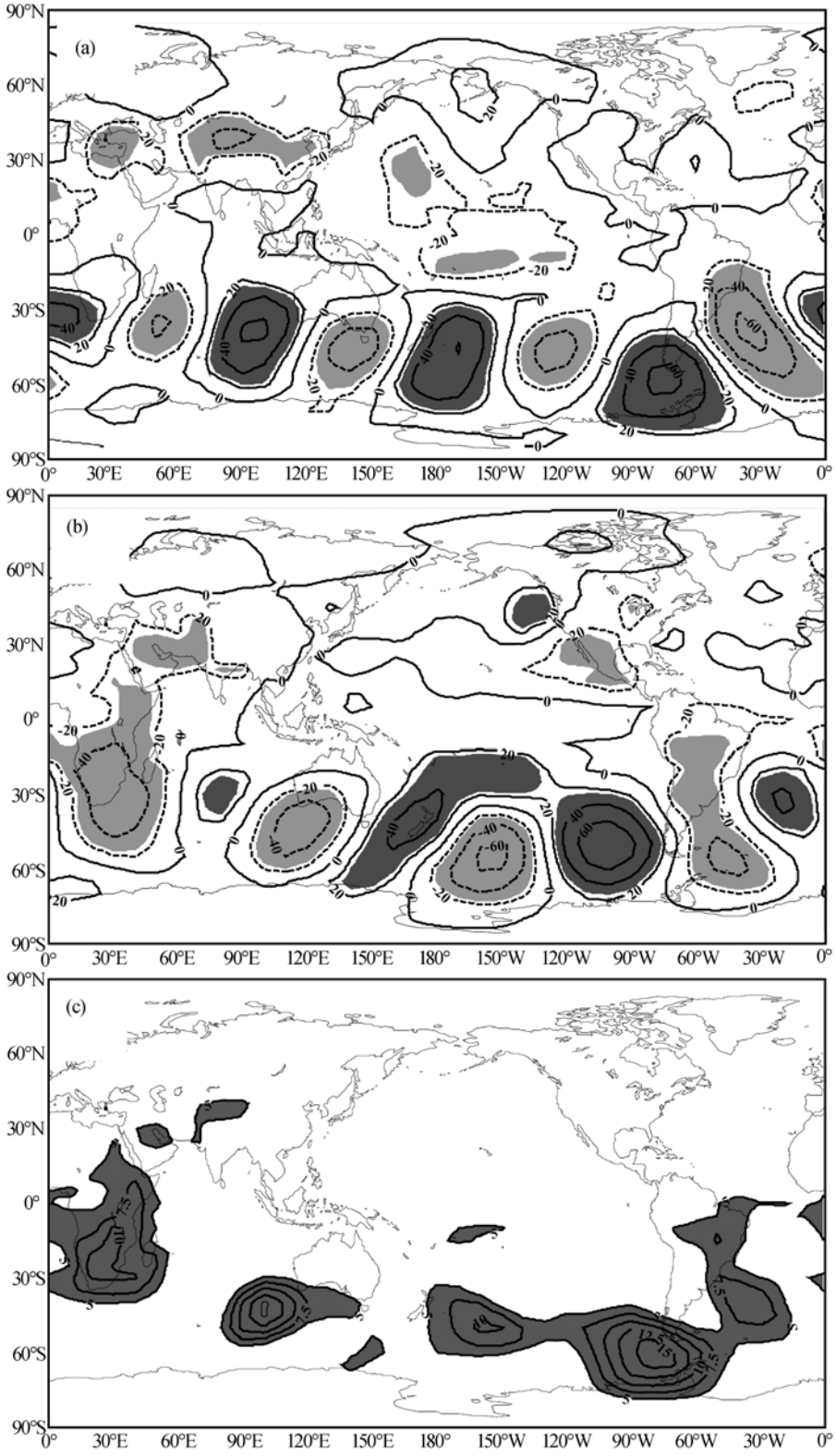

Figure 4 The spatial distribution of the first principal 20—30-day oscillation pattern (POP1, SCGT) for the global 850 hPa low-frequency height anomalies in May—August during the period of 1979—2005: real part (a), imaginary part (b), spatial distribution (c) of explained variances to the total variability. In (a) and (b),values are multiplied by 1000 and darker (light) grey shaded areas represent the regions greater than 25 (less than −25). In (c), values (unit: %) are multiplied by 100 and the contours greater than 5 are shaded.

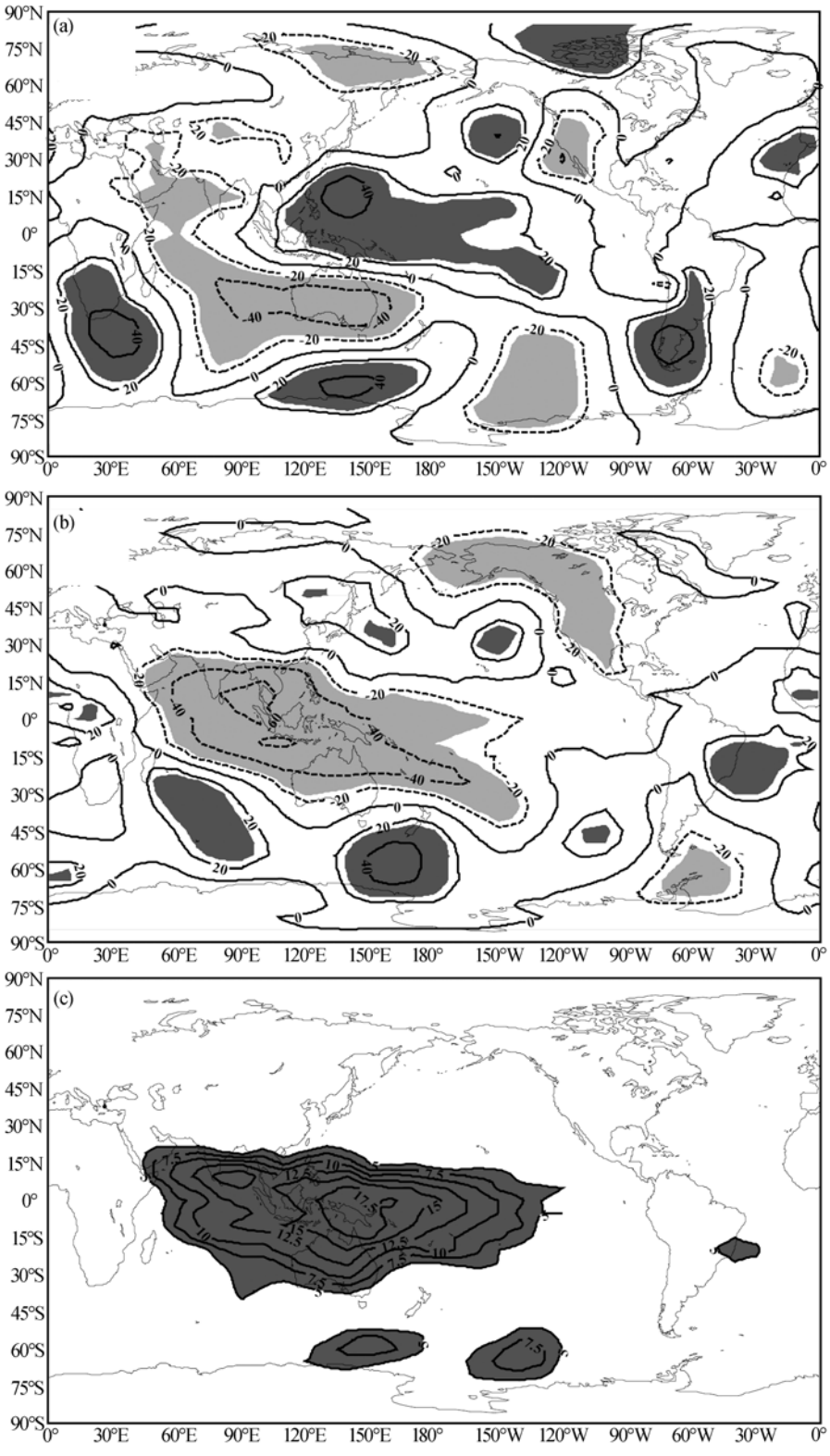

Figure 5 Same as Figure 4 but for the second principal 20—30-day oscillation pattern (POP2, TWP).

alternatively from the middle latitudes of East Asia via subtropical East Asia and tropical Indian Ocean, western Pacific to southern subtropical Indian Ocean and Australia. In evolution of this model, the significant active regions are over the tropical eastern Indian Ocean and western Pacific and the maximum value of explained

variance is up to 18% (Figure 5(c)). It is also seen from the POP cycle that a low frequency wave train moves southward from the western subtropical Pacific into the southern subtropical Indian Ocean and Australia, which is developed and up to peak phase over the western tropical Pacific (Figure 5(b)). This ISO signal is referred to as the tropical western Pacific (TWP) pattern. The evolution of this low-frequency wave train is closely related to the heating anomalies and air-sea interaction in South Asia and East Asia. It directly affects the summer monsoon rainfall in East Asia.

Meanwhile, the evolution of the composite low frequency 850 hPa geopotential height for the eight phases of the POP cycle also demonstrates that the eastward propagation of SCGT and the southward propagation of TWP are evident (not shown). In addition, the simultaneous correlation between imaginary (real) time coefficient of POP1 (POP2) and low frequency rainfall over LYRV on the time scale of 20—30-day is 0.178 (0.206), which has a significance at 95% (98%) confidence level with the effective number of independent samples of 133 days. It further confirms the existence of a strong relationship of the rainfall ISO over LYRV to SCGT (POP1) or TWP (POP2). Therefore, the global principal ISO patterns are dominated by the eastward propagating SCGT and southward propagating TWP pattern in the Northern Hemisphere summer, respectively. These two ISO patterns play more important roles in the circulation and rainfall in South Asia and East Asia and the middle latitude in the Southern Hemisphere on the time scale of 20—30 days. As such, the POP prediction models are set up by these two ISO patterns, which may predict well the evolutions of the principal low frequency flow patterns related to the 20—30-day oscillation of rainfall over LYRV.

Furthermore, probabilities are also statistically determined of the occurrence of the heavy precipitation process over LYRV in the POP cycle corresponding to the SCGT or TWP pattern in May—August over the 27 years. The results are presented as follows. The probabilities are 54.9% and 60.4%, respectively, within the positive phase of imaginary part of POP1 and real part of POP2. A χ^2 test is conducted of the statistic result with and without the heavy precipitation process for the 20—30-day oscillation of SCGT or TWP pattern. The results show significant differences at the significance level of 95% and 99%, respectively. This indicates that it is reliable to use the 20—30-day oscillations corresponding to SCGT and TWP pattern to make extended-range forecast whether the heavy precipitation process will appear over LYRV for the 10—30 days in the further.

3.3 Global circulation models with and without the heavy precipitation process over LYRV

According to above analysis, both SCGT and TWP patterns of the global 20—30-day oscillation modulate simultaneously the heavy precipitation process over LYRV. To make full use of these 20—30-day oscillations, the cases with and without the heavy precipitation process over LYRV for May, June, July and August are selected to set up two kinds of the global atmospheric circulation models for the heavy precipitation process by composing phases of the ISO patterns. And the differences between these two circulation patterns and their evolutions can be understood better to serve the extended-range forecasting for the 10—30 days. The amplitude and phase information of the POP pattern associated with SCGT or TWP pattern are given from the complex time series $z(t)=z_r(t)+jz_i(t)$, ($j=\sqrt{-1}$), i.e., $A(t)=\sqrt{z_r(t)^2+z_i(t)^2}$ and $\theta(t)=\tan^{-1}[z_i(t)/z_r(t)]$, which indicate the active component of the wave through eight phases, 1—8, corresponding to θ_i э (7π/8, 9π/8), (5π/8, 7π/8), (3π/8, 5π/8), (π/8, 3 π/8), ⋯, (–7π/8, –5π/8) (i=1, 2, ⋯, 8). For the global 850 hPa low frequency wind, the evolutions of ISO patterns with and without the heavy precipitation process over LYRV are obtained by the composite analysis, respectively. In these composite analyses, a 20—30-day oscillation is considered a process in which the amplitude anomaly is larger than 0.5 standard deviation, and the cycle consists of: $\cdots\rightarrow\theta_1\rightarrow\theta_2\rightarrow\theta_3\rightarrow\theta_4\rightarrow\theta_5\rightarrow\theta_6\rightarrow\theta_7\rightarrow\theta_8\rightarrow\theta_1\rightarrow\cdots$.

Figure 6(a)—(h) gives the distribution of the global 850 hPa composite low-frequency wind field for eight phases of POP1 (SCGT) with the heavy precipitation process over LYRV. Consistent with the 850 hPa geopotential height field (Figure 4(a) and (b)), there is a predominant circumglobal teleconnection wave train over the middle latitude of the Southern Hemisphere in entire cycle. This wave train is associated with a slow eastward propagating of the alternating cyclonic/anticyclonic/cyclonic circulation patterns on the time scale of 20—30

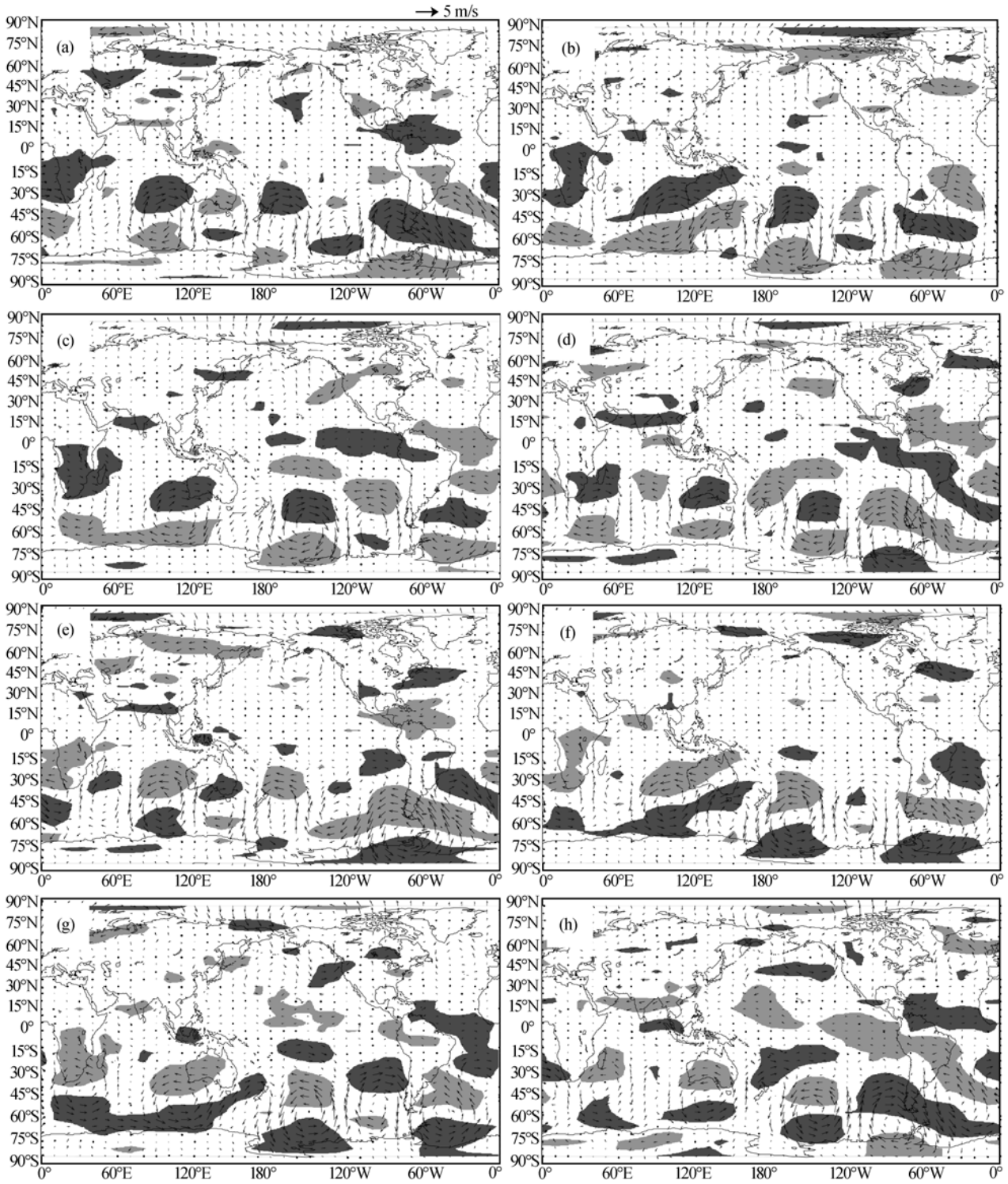

Figure 6 The distribution of the global 850 hPa composite wind field ((a)—(h)) for eight phases of SCGT (θ_1, θ_2, ⋯, θ_7, θ_8) with the heavy precipitation process over LYRV in association with the 20—30-day oscillation. Vector anomalies (unit: m/s) at the 95% *t*-test confidence level in *u*-component anomaly are shaded.

days. On the other hand, for the evolution of OLR, there is a low frequency wave train with signs changing alternatively from the middle latitude of the southern Indian Ocean through the tropical Indian Ocean and Arabian Sea to central Asia (Figure 7(a)—(h)). This spatial wave intensifies up to peak state in Phase 4 (Figure 7(d))

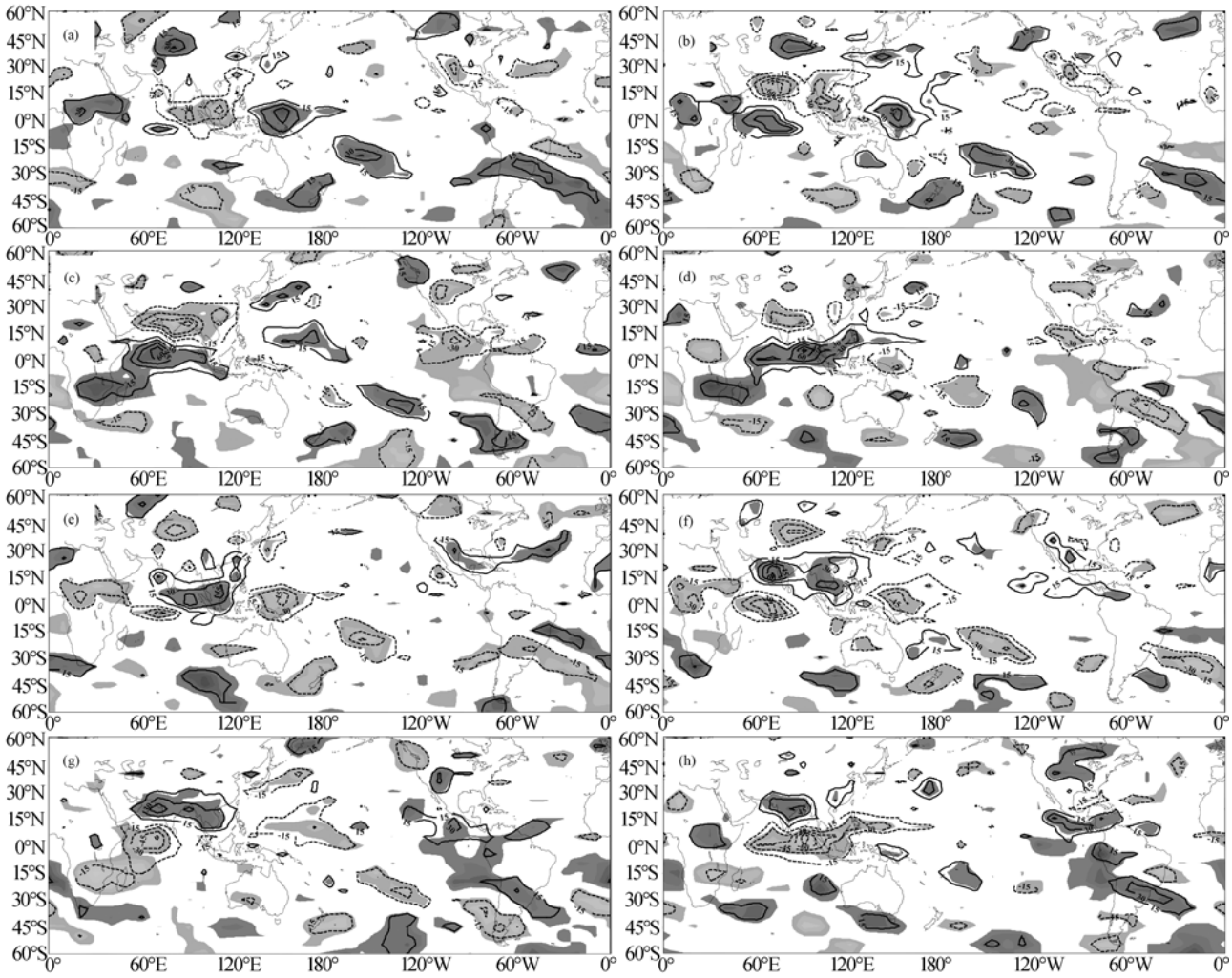

Figure 7 Same as Figure 6 but for the low-frequency OLR anomalies (unit: 0.1 $W \cdot m^{-2}$) over the global low-middle latitudes. Above 95% confidence level is shaded.

and Phase 8 (Figure 7(h)). It is reflected that the interaction between the convection activity in the tropical Indian Ocean and South Asia and the low-frequency wavetrain in the extratropics of the Southern Hemisphere on the time scale of 20—30 days. The point to note is that a strong westerly (easterly) stream appears from the Arabian Sea via India and BOB to southern China and LYRV in Phase 4 (Figure 6(d)) and Phase 8 (Figure 6(h)). Such a strong westerly stream is closely related to the quick developing of the convective heating patterns with the north-south dipole structure over the tropical Indian Ocean and South Asia from Phase 3 to Phase 4 (Figure 7(c)—(d)). And in Phase 4, the heavy precipitation process over LYRV occurs primarily (Figure 6(d)). In this phase, there are the significant negative areas (enhanced convection activity) over LYRV and the Yangtze-Huaihe valley for the spatial distributions of OLR (Figure 7(d)), corresponding to the stronger moisture transport from India into East Asia in the lower troposphere[41]. It suggests the indirect influence of the variations of westerly jet stream in the middle latitude of the Southern Hemisphere on the rainfall over LYRV. Conversely, such a strong westerly stream disappears for the case without the heavy precipitation process over LYRV associated with the weaker moisture transport for Phase 4 (Figure 8(b)). In this case, SCGT still exists in the middle latitude of the Southern Hemisphere (Figure 8(a) —(d)). But, its intensity is weakened, corresponding to the weak wave train of OLR (not shown). The moisture transport of southwest monsoon in India is one of the most important factors influencing the heavy precipitation process over LYRV. Thus, the rainfall over LYRV is decreased to be attributed to the weaker westerly stream from the Arabian Sea via India and BOB to southern China and LYRV on the time scale of 20—30 days.

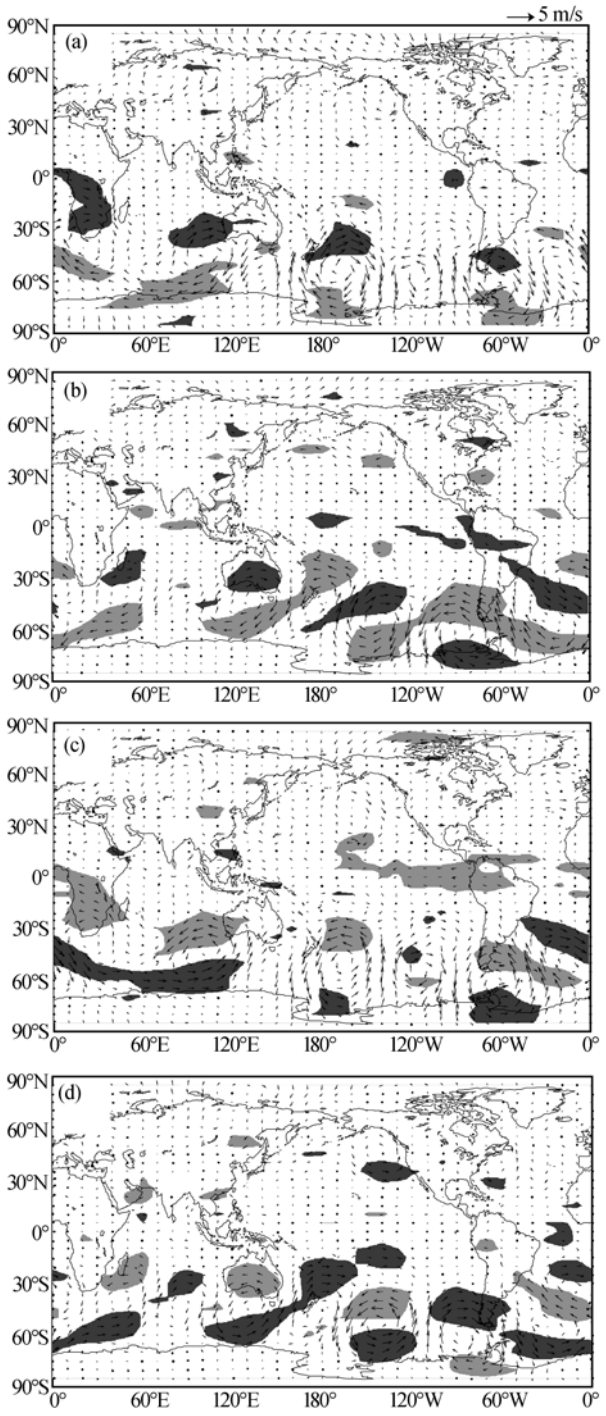

Figure 8 Same as Figure 6 but for the case without the heavy precipitation process over LYRV for four phases. (a) θ_2; (b) θ_4; (c) θ_6; (d) θ_8.

Clearly, there is indication of the weak interaction in both hemispheres associated with suppressed convection activity in the tropical Indian Ocean.

For another principal ISO pattern, i.e., POP2 (TWP), there is a pronounced southward propagation of the low-frequency cyclone and anticyclone circulations from the middle latitude of East Asia through tropical western Pacific to southern subtropical Indian Ocean and Australia with the heavy precipitation process, as shown in Figure 9(a)—(h). In this cycle, most of the heavy precipitation processes over LYRV appear in Phase 6 (Figure 9(f)). The distinct feature of this phase is that a broad belt of the strong westerly wind anomaly is located near 20°—30°N from India via BOB to LYRV and subtropical northwestern Pacific and central and eastern equatorial Pacific. Meantime, the low-frequency anticyclone and cyclone circulation appear in the Philippines and the east coast of Japan, respectively. In contrast, this belt of the westerly wind anomaly is weaker, and there is no clear signature of the wind anomaly over India and BOB without the heavy precipitation process over LYRV for Phase 6 (Figure 10(c)). As a result, the moisture transports at 850 hPa over LYRV are decreased and do not favor maintaining the heavy precipitation processes. At the same time, the moving of the low frequency cyclone for the TWP pattern shifts somewhat westward in the cycle (Figure 10(a)—(d)). Apparently, the spatial structure and propagation path of the TWP pattern directly influence the forming of the heavy precipitation process over LYRV.

As mentioned above, when the positive phases of 20—30-day oscillation for the rainfall over LYRV are associated with (without) the heavy precipitation process, a strong westerly stream appears (disappears) from the Arabian Sea via India and BOB to southern China and LYRV for the global 850 hPa filtered wind field during Phase 4 of SCGT. This situation is favorable (unfavorable) for the forming of the heavy precipitation process over LYRV. In a similar manner, a strong (weak) western wind belt forms from India through BOB to southern China and LYRV and the subtropical northwestern Pacific and central and eastern equatorial Pacific during Phase 6 of TWP for the cases with (without) the heavy precipitation process. These two models can reflect well the difference of the global atmospheric circulations between with and without the heavy precipitation process over LYRV. The forming and maintaining of the heavy precipitation processes over LYRV are modulated simultaneously by both SCGT and TWP on the time scale of 20—30 days. These global principal ISO patterns are excited by either the interaction of the extratropical circulation in both hemispheres or the heat

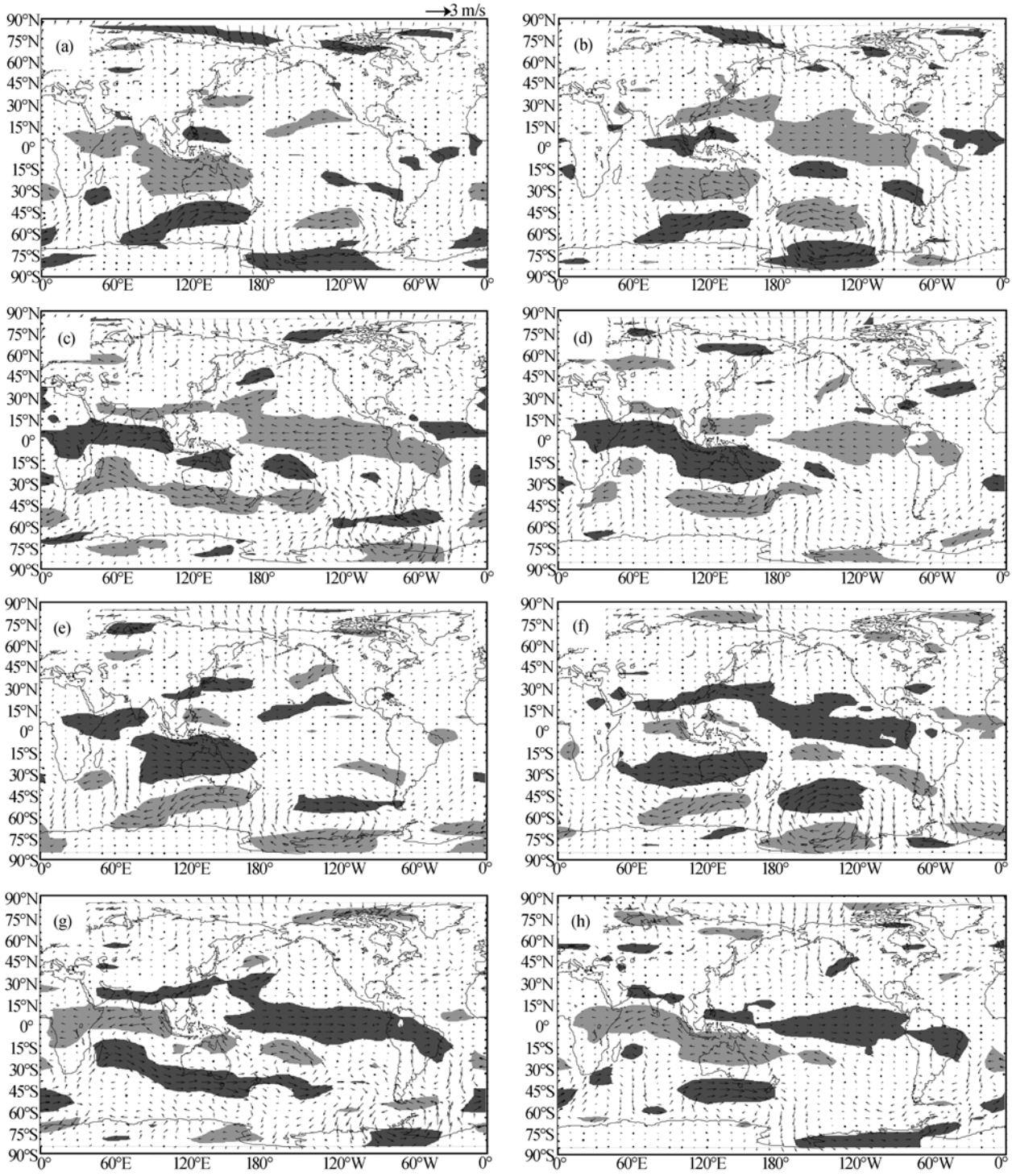

Figure 9 The distribution of the global 850 hPa composite wind field ((a)—(h)) for eight phases of TWP (θ_1, θ_2, ⋯, θ_7, θ_8) with the heavy precipitation process over LYRV in association with the 20—30-day oscillation. Vector anomalies (unit: m/s) at the 95% *t*-test confidence level in *u*-component anomaly are shaded.

source forcing in Asia monsoon domain and the internal interaction of circulation in East Asia. One important result is that the 20—30-day oscillation of the rainfall and circulation associated with the heavy precipitation process over LYRV cannot be considered as an independent process within the East Asian summer monsoon. It is clear that these 20—30-day oscillations of the rainfall over LYRV are not only influenced by the systems

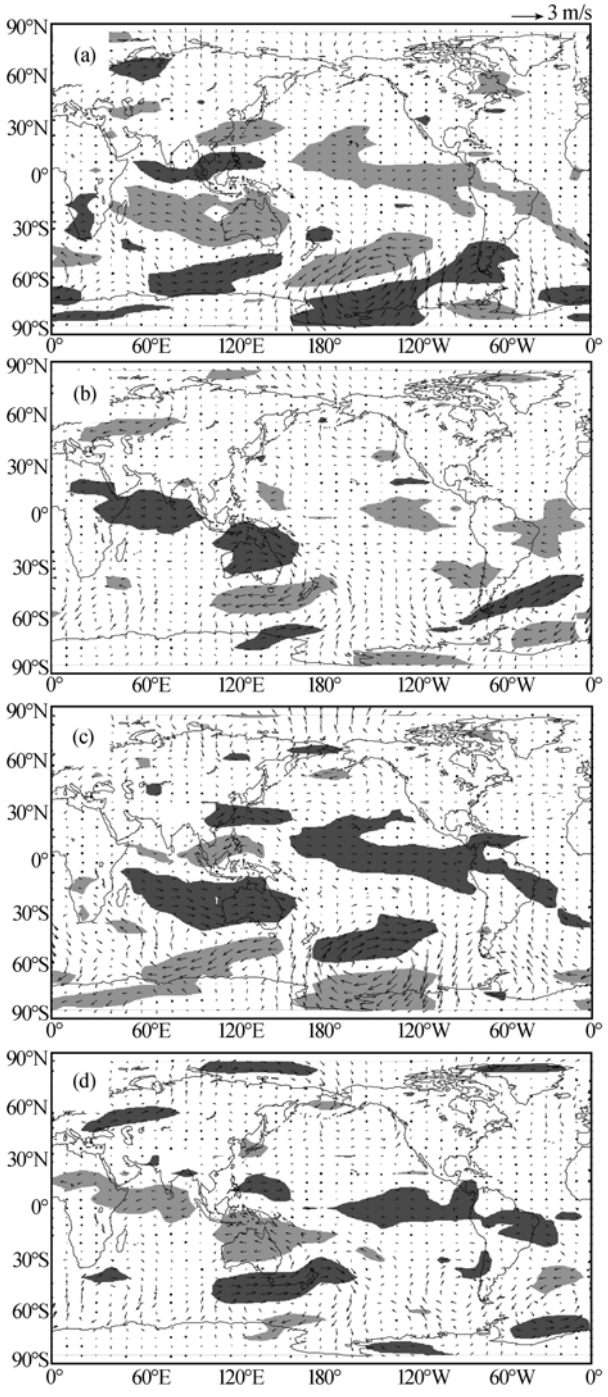

Figure 10 Same as Figure 9 but for the case without the heavy precipitation process over LYRV for four phases. (a)θ_2; (b) θ_4; (c) θ_6; (d) θ_8.

in the Asian monsoon domain but are also affected to some extent by the activity of the mid-latitude ISO in the Southern Hemisphere. Hence, the heavy precipitation process over LYRV cannot be studied in isolation when attempting to understand the key processes that may be responsible for its variability.

4 Conclusions

By using the methods of the non-integer spectrum analysis, correlation analysis, POP analysis, and composition analysis, we analyzed the variations of low-frequency oscillation of the daily rainfall over LYRV and the connections between the heavy precipitation process and principal ISO oscillation patterns of the global circulation in May—August from 1979 to 2005, and discussed the possible mechanisms. We have drawn the following conclusions:

(1) In May—August, the variation of the daily rainfall over LYRV is mainly of oscillations of 10—20, 20—30 and 60—70 days, in which the interannual variation of the intensity of its 28-day oscillation has a strongly positive correlation with the number of the heavy precipitation process over LYRV.

(2) Two modes (POP1, POP2) are revealed by POP for the 20—30-day oscillation of the global 850 hPa circulation. One is a circumglobal teleconnection wave train in the middle latitude of the Southern Hemisphere (SCGT) with an eastward propagation, and the other is the southward propagation pattern in the tropical western Pacific (TWP). The POP modes explain 7.72% and 7.66% of variance, respectively. These two principal ISO patterns are closely related to the low frequency rainfall and heavy precipitation process over LYRV, in which the average probability for the heavy precipitation process over LYRV is 54.9% and 60.4% for the positive phase of imaginary part of POP1 and real part of POP2, respectively. The former is a teleconnection between SCGT and low frequency rainfall over LYRV, which is associated with the heating in the tropical Indian Ocean and the interaction of circulations in both hemispheres; while the latter is reflected by the direct influence of TWP in tropics, which is closely linked to the heating in the tropical western Pacific and internal nonlinear interaction of the circulations in East Asia.

(3) The models of the global atmospheric circulation for the 20—30-day oscillation in association with or without the heavy precipitation process over LYRV in May—August are set up by means of the composite analysis method. Most of the heavy precipitation processes over LYRV appear in Phase 4 of SCGT or Phase 6 of TWP. When the positive phases of the 20—30-day oscillation for the rainfall over LYRV are associated with (without) the heavy precipitation process, a strong

westerly stream appears (disappears) from the Arabian Sea via India and BOB to southern China and LYRV for the global 850 hPa filtered wind field during the Phase 4 of SCGT. This situation is favorable (unfavorable) for the forming of the heavy precipitation process over LYRV. In a similar way, a strong (weak) western wind belt forms from India through BOB to southern China and LYRV and the subtropical northwestern Pacific and central and eastern equatorial Pacific during the Phase 6 of TWP for the cases with (without) the heavy precipitation process. These two global circulation models can reflect well the difference of atmospheric circulations between with and without the heavy precipitation process over LYRV, and will be helpful to the prediction of the summertime heavy precipitation process over LYRV for the extended-range forecasting during the 10－30 days.

The author thanks all peer-reviewers concerned for their valuable comments in revising the current paper.

1 Madden R A, Julian P R. Detection of a 40－50 day oscillation in the zonal wind in the tropical Pacific. J Atmos Sci, 1971, 28: 702－708

2 Madden R A, Julian P R. Description of global-scale circulation cells in the tropics with a 40－50-day period. J Atmos Sci, 1972, 29: 1109－1123

3 Madden R A, Julian P R. Observation of the 40－50-day tropical oscillation —— A review. Mon Weather Rev, 1994, 122: 814－837

4 Zhang C D. Madden-Julian oscillation. Rev Geophys, 2005, 43: RG2003, doi: 10.1029/2004/RG000158

5 Maloney E D, Hartmann D L. Modulation of hurricane activity in the Gulf of Mexico by the Madden-Julian oscillation. Science, 2000, 287: 2002－2004

6 Ding Q H, Wang B. Intraseasonal teleconnection between the summer Eurasian wave train and the Indian monsoon. J Clim, 2007, 20(15): 3751－3767

7 Guan B, Johnny C L C. Nonstationarity of the intraseasonal oscillations associated with the western North Pacific summer monsoon. J Clim, 2006, 19(4): 622－629

8 Matthews A J, Li H Y. Modulation of station rainfall over the western Pacific by the Madden-Julian oscillation. Geophys Res Lett, 2005, 32: L14827, doi: 10.1029/2005GL023595

9 Goswami B N, Wu G X, Yasunari T. The annual cycle, intraseasonal oscillations, and roadblock to seasonal predictability of the Asian summer monsoon. J Clim, 2006, 19(20): 5078－5099

10 Kim B M, Lim G H, Kim K Y. A new look at the midlatitude-MJO teleconnection in the northern hemisphere winter. Q J R Meteorol Soc, 2006, 132: 485－503

11 Krishnamurthy V, Shukla J. Seasonal persistence and propagation of intraseasonal patterns over the Indian monsoon region. Clim Dyn, 2008, 30(4): 353－369

12 Carvalho L M V, Jones C, Ambrizzi T. Opposite phases of the Antarctic Oscillation and relationships with intraseasonal to interannual activity in the tropics during the austral summer. J Clim, 2005, 18: 702－718

13 Li C Y. Recent progress in atmospheric intraseasonal oscillation research (in Chinese). Prog Nat Sci, 2004, 14(7): 734－741

14 Wang H J, Han J P, Zhang Q Y, et al. Brief review of some CLIVAR-related studies in China. Adv Atmos Sci, 2007, 24(6): 1037－1048

15 Huang R H, Zhou L T, Chen W. The progress of recent studies on the variability of the East Asian monsoon and their causes. Adv Atmos Sci, 2003, 20(1): 55－69

16 Han R Q, Li W J, Dong M. Impacts of 30－60-day oscillations over the subtropical Pacific on the East Asian summer rainfall. Acta Meteorol Sin, 2006, 20(4): 459－474

17 Takayabu Y N, Iguchi T, Kachi M, et al. Abrupt termination of the 1997－98 El Niño in response to a Madden-Julian oscillation. Nature, 1999, 402: 279－282

18 Mao J Y, Wu G X. Intraseasonal variability in the Yangtze-Huaihe River rainfall and subtropical high during the 1991 Meiyu period (in Chinese). Acta Meteorol Sin, 2005, 63(5): 762－770

19 He J H, Li J, Li Y P. Nnumerical experiment with processes for effect of Australian cold air activity on East-Asian summer monsoon (in Chinese). Acta Meteorol Sin, 1991, 49(2): 162－169

20 Waliser D E, Lau K M, Stern W, et al. Potential predictability of the Madden-Julian oscillation. Bull Amer Meteorol Soc, 2003, 84(1): 33－50

21 Waliser D E, Stern W, Schubert S, et al. Dynamical predictability of intraseasonal variability associated with the Asian summer monsoon. Q J R Meteorol Soc, 2003, 129: 2897－2925

22 Waliser D E, Jones C, Schemm J K, et al. A statistical extended-range tropical forecast model based on the slow evolution of the Madden-Julian oscillation. J Clim, 1999, 12: 1918－1939

23 Weickmann K, Berry E. A synoptic-dynamic model of subseasonal atmospheric variability. Mon Weather Rev, 2007, 135(2): 449－474

24 Webster P J, Hoyos C. Prediction of monsoon rainfall and river discharge on 15－30 day time scales. Bull Amer Meteorol Soc, 2004, 85: 1745－1765

25 Jones C, Carvalho L M V, Higgins W, et al. A statistical forecast model of tropical intraseasonal convective anomalies. J Clim, 2004, 17: 2078－2095

26 Maharaj E A, Wheeler M C. Forecasting an index of the Madden-Julian oscillation. Int J Climatol, 2005, 25: 1611－1618

27 Xavier P K, Goswami B N. An analog method for real-time forecasting of summer monsoon subseasonal variability. Mon Weather Rev, 2007, 135(12): 4149－4160

28 Miura H, Satoh M, Nasuno T, et al. A Madden-Julian oscillation event realistically simulated by a global cloud-resolving model. Science, 2007, 318: 1763－1765

29 Zhang Q Y, Tao S Y, Zhang S L. The persistent heavy rainfall over

the Yangtze River valley and its associations with the circulations over East Asia during summer (in Chinese). Chin J Atmos Sci, 2003, 27(6): 1018－1030
30 Wang B, Webster P J, Kikuchi K, et al. Boreal summer quasi-monthly oscillation in the global tropics. Clim Dyn, 2006, 27: 661－675
31 Simmons A J. The forcing of stationary wave motion by tropical diabatic heating. Q J R Meteorol Soc, 1982, 108: 503－534
32 Kalnay E, Kanamitsu M, Kistler R, et al. The NCEP-NCAR 40-year reanalysis project. Bull Amer Meteorol Soc, 1996, 77: 437－471
33 Schickedanz P T, Bowen E G. The computation of climatological power spectra. J Appl Meteorol, 1977, 16: 359－367
34 Hasselmann K. PIPs and POPs: The reduction of complex dynamical systems using principal interaction and oscillation patterns. J Geophys Res, 1988, 93D: 11015－11021
35 von Storch H, Bu¨rger G, Schnur R, et al. Principal oscillation patterns: A review. J Clim, 1995, 8: 377－400
36 Yang Q M. Interdecadal variations of connections between the principal biennial oscillation pattern of rain in China and global 500 hPa circulation (in Chinese). Chin J Atmos Sci, 2006, 30(1): 131－145
37 Chen W Y. Fluctuations in the Northern Hemisphere 700 hPa height field associated with the Southern Oscillation. Mea Weather Mon, 1982, 110: 808－823
38 Murakami M. Large-scale aspects of deep convective activity over the GATE area. Mon Weather Rev, 1979, 107: 994－1013
39 Ghil M, Kingtse M. Intraseasonal oscillations in the global atmosphere. Part II: Southern Hemisphere. J Atmos Sci, 1991, 48: 780－790
40 Ambrizzi T, Hoskins B J, Hsu H H. Rossby wave propagation and teleconnection in the austral winter. J Atmos Sci, 1995, 52: 3661－3672
41 Zhou X X, Ding Y H, Wang P X. Moisture transport in Asian summer monsoon region and its relationship with summer precipitation in China (in Chinese). Acta Meteorol Sin, 2008, 66(1): 59－70